IMPEDANCE ESTIMATES AND REQUIREMENTS FOR THE PS2*

V. Lebedev[#], FNAL, Batavia, IL 60510, U.S.A.

Abstract

The small ring impedance required for beam stability and the fast ramping rate required to boost the integrated particle flux in a fast ramping syncrotron are contradictory to each other. The paper discusses possible aproaches to the choice of PS-2 vacuum chamber and major limitations on the ring impedance and the beam stability.

1. RING PARAMETERS

There is a similarity between PS-2 parameters and parameters of FNAL's Project-X [1]. Both projects are based on the multi-turn injection from a SC linac. Unlike the PS-2 which will be a new ring in CERN, FNAL plans to upgrade the existing Main Injector (MI) for Project X The MI has higher injection and extraction energies than are presently considered for the PS-2. Parameters for both synchrotrons are presented in Table 1.

Table 1: Tentative PS-2 and MI parameters

	FNAL MI		PS-2
	Present	Project X	
Injection energy, GeV	8		5
Extraction energy, GeV	120(max. 150)		50
Circumference, m	3319.42		1346
Particles per bunch	$0.7\cdot10^{11}$	$3.1\cdot10^{11}$	$4\cdot10^{11}$
Beam current at inj., A	0.49	2.45	2.5
Cycle duration, s	2.2	1.4	1.5
Norm. 95% emit., mm mrad	15/15	25/25	18
Norm. acceptance at inj., mm mrad	40/40	40/40	100
90% long.emit., eV s/bunch	0.4	0.5	0.5
Total number of particles	$3.4\cdot10^{13}$	$1.7\cdot10^{14}$	$6.5\cdot10^{13}$
Betatron tunes, Q_x/Q_y	26.42/ 25.41	26.45/ 25.46	~15
Maximum Coulomb tune shifts, $\Delta Qx/\Delta Qy$	0.033/ 0.038	0.043/ 0.046[1]	0.07/ 012
Harmonic number	588	588	180
Accelerating freq., MHZ	53	53	40

2. MAGNETIC FIELD SCREENING BY VACUUM CHAMBER

To achieve reliable operation of the synchrotron with the required beam current it is highly desirable to reduce the ring impedances. That is normally achieved by minimizing the number of discontinuities of the vacuum chamber and making the vacuum chamber from high conductive material (aluminum, copper). Nevertheless the high conductivity of the walls results in the magnetic field screening by the vacuum chamber walls due to eddy currents. For the planned ramping frequency (f~0.5-0.3 Hz) the skin-depth in the vacuum chamber walls, δ, is much larger than the wall thickness, d, and the correction to the dipole magnetic field in the vacuum chamber center is:

$$\left.\frac{\delta B}{B}\right|_y = i\frac{a_x d}{\delta^2}F(a_x,a_y) \quad . \qquad (1)$$

For elliptic vacuum chamber with half sizes a_x and a_y and the constant thickness of the wall, $d << a_x$, a_y, the form-factor in Eq. (1) is equal to:

$$F(a_x,a_y)=\frac{4a_y}{\pi}\int_0^{\pi/2}\frac{\sqrt{a_x{}^4\sin\varphi+a_y{}^4\cos\varphi}}{\left(a_x{}^2\sin\varphi+a_y{}^2\cos\varphi\right)^{3/2}}(\cos\varphi)^2\,d\varphi \quad . \qquad (2)$$

One can see that it depends only on the ratio of the sizes, $x=a_x/a_y$. Figure 1 presents corresponding plot.

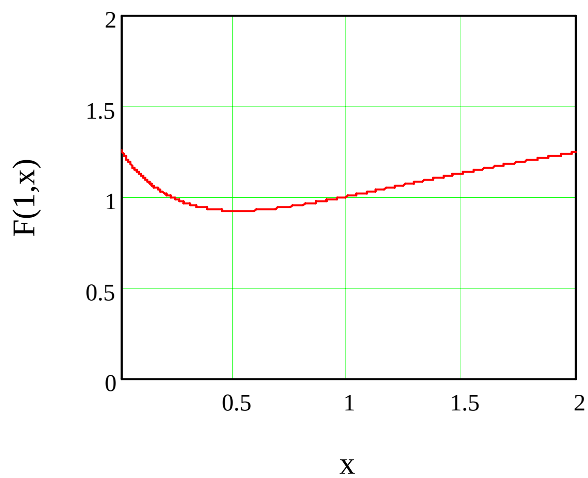

Figure 1. Dependence of Eq. (1) form-factor on the ratio of vacuum chamber sizes, $x = a_x / a_x$.

The vacuum chamber sizes are set by the machine acceptances. For the maximum of beta-function of ≈40 m and the normalized acceptances: $\varepsilon_{xn} \approx \varepsilon_{yn} \approx$ 100 mm mrad one obtains typical sizes: $a_x \approx$ 6.2 cm, $a_y \approx$ 2.5cm (horizontal size is increased to accept of momentum particles). Those are the same dimensions as for FNAL MI. It is expected that the actual PS-2 vacuum chamber will be very similar. For stainless steel with d = 1.3 mm (FNAL MI) and f = 1 Hz one obtains $\delta B/B \approx 2\cdot10^{-4}$. Aluminum is less rigid material and should have thicker walls. For d = 3 mm one obtains $\delta B/B \approx 10^{-2}$ which is too large value to be accepted for a fast cycling synchrotron. The problem is exacerbated by the fact that the field is not-uniform across the aperture as shown in Figure 2.

Note that if the field correction would be constant across the aperture its value could be easily corrected by

* Work supported by Fermi Research Alliance, LLC., under contract DE-AC02-76CH03000 with the U.S. Dept. of Energy.
[#]val@fnal..gov

[1] Flat transverse and longitudinal distributions are achieved by painting the small emittance linac beam at injection to synchrotron.

minor adjustment of the quad currents relative to the dipole current. The uniformity of field correction can be achieved by using a vacuum chamber with specially profiled thickness so that the inner and outer boundaries are similar ellipses, $\Delta a_x / a_x \equiv \Delta a_y / a_y$. In this case the field correction is:

$$\frac{\delta B}{B} = i\frac{2a_x a_y \Delta a_x}{\delta^2 (a_x + a_y)} \quad , \qquad (3)$$

and it is uniform across the aperture.

Figure 2 presents comparison of field variation along *x*-axis for the cases of equal wall thickness and similar elliptic boundaries. Such a choice, in principle, allows one to use an extruded aluminum vacuum chamber which is inexpensive to manufacture. Nevertheless to have a good uniformity of the field correction one needs to have high accuracy in the chamber profile, and uniformity of material (no cracks, etc.). Although such a choice does not look too attractive from operational point of view, because of the imbalance in the quad and dipole magnetic fields, it could significantly reduce resistive wall impedance. Note that the field correction inside quads is non–uniform with the exception of the round vacuum chamber case.

3. TRANSVERSE IMPEDANCE DUE TO WALL RESISTIVITY

For an estimate of the transverse impedance, we will use the expression describing the transverse impedance of a round vacuum chamber (see details in Ref. [2]) ($d << a$, $b = a + d$):

$$Z_\perp = -i\frac{Z_0(2\pi R)}{2\pi a^2}\left[\frac{2e^{kd}(1+kb) - e^{-kd}(1-kb)}{e^{kd}(1+ka)(1+kb) - e^{-kd}(1-ka)(1-kb)} + \frac{1}{\beta} - 1\right], \qquad (4)$$

where a and b are the inner and outer radii of the chamber, R is the ring radius, Z_0=377 Ω, $k = (1-i)/\delta$, and βc is the beam velocity. Its asymptotical behavior can be presented by the following expression:

$$Z_\perp = (2\pi R) Z_0 \begin{cases} \dfrac{c(1-i)}{2\pi a^3\sqrt{2\pi\sigma_R \omega}} - \dfrac{i}{2\pi a^2}\left(\dfrac{1}{\beta} - 1\right) & , \quad \delta \le d \\ \dfrac{c^2}{4\pi^2 \sigma_R \omega a^3 d} - i(\ldots) & , \quad \sqrt{ad} \ge \delta \ge d \\ \dfrac{\sigma_R \omega d}{c^2 a} - i\dfrac{1}{2\pi a^2 \beta} & , \quad \delta \ge \sqrt{ad} \end{cases} \qquad (5)$$

The corresponding plot for the expected PS-2 resistive wall impedance is presented in Figure 3. One can see that at the lowest betatron sideband accounting the finite thickness of the vacuum chamber results in small correction (~20-30%) for the resistive part of the impedance and in the most of cases can be neglected. Consequently, an approximation of $\delta < d$ (top equation in Eq. (5)) can be used for the impedance calculations. The impedance of elliptical vacuum chamber with large ratio of sizes, a_x/a_y>>1, is close to the impedance of a flat vacuum chamber. In this case the resistive part of vertical impedance is $\pi^2/12 \approx 0.822$ times smaller than the resistive part of impedance for round vacuum chamber with the radius equal to the half gap [3]. The horizontal impedance is half of the vertical one.

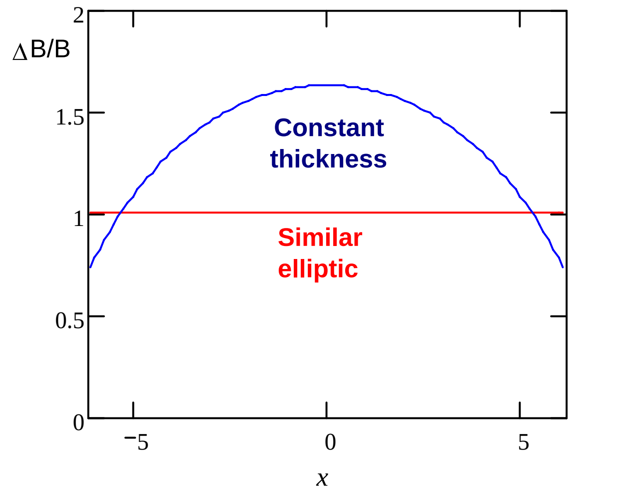

Figure 2. Dependence $\Delta B_y(x,0)$ for similar elliptic and constant width vacuum chambers, arbitrary units, $a_x \approx 6.2$ cm, $a_y \approx 2.5$cm, $\Delta a_x = d$.

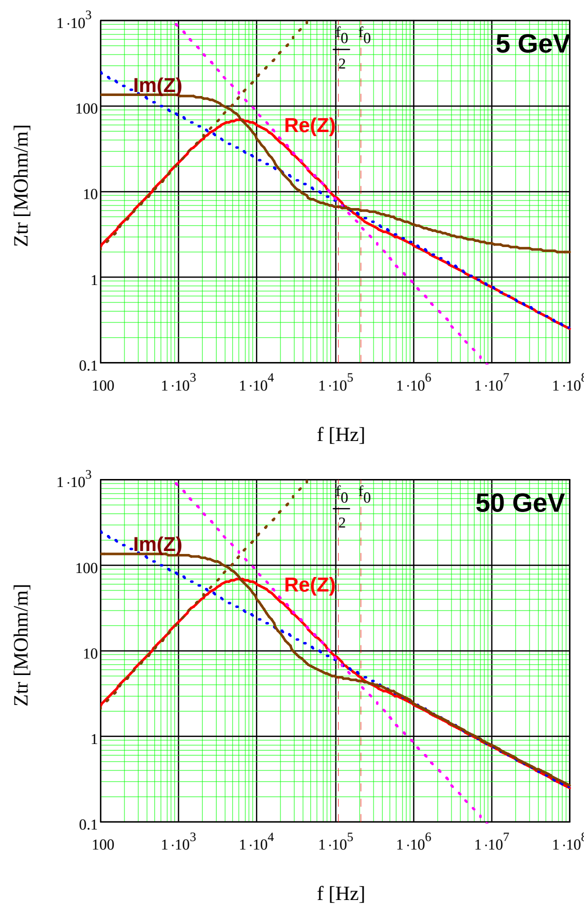

Figure 3. Transverse impedance per unit length of round stainless steel vacuum chamber, r = a = 25 mm, d=1.3 mm; top - 5 GeV, bottom - 50 GeV.

A detailed analysis carried out for Tevatron [4] showed that in the case of stainless steel vacuum chamber the impedance is dominated by wall resistivity at frequencies below ~100 MHz. With a properly built vacuum chamber the similar relationship should be justified for the PS-2 vacuum chamber.

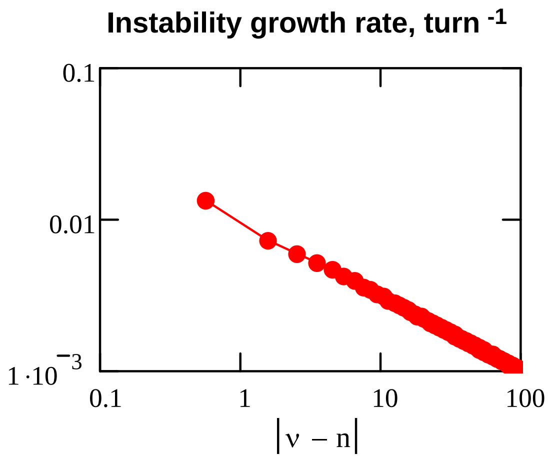

Figure 4. Instability growth rate for different transverse modes at the injection energy of PS-2.

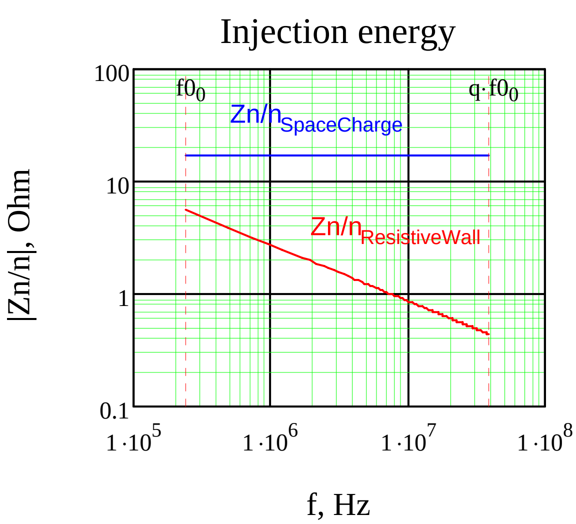

Figure 5. Dependence of the space charge and resistive wall longitudinal impedances on frequency for the PS-2 parameters and stainless steel vacuum chamber.

To estimate an effect of ring impedance on the transverse beam stability we consider the betatron tune shift due to the wall resistivity where we will be using the top equation of Eq. (5) for the impedance and the mentioned above $\pi^2/12$ correction for flat vacuum chamber. That results in:

$$\Delta\nu_{y_n} = -\frac{1+i}{96\pi}\frac{r_p(I_0/e)(2\pi R)^{5/2}}{\gamma\beta^2 \nu a_y{}^3\sqrt{\sigma_R c(n-\nu)}} \quad , \qquad (6)$$

where ν is the betatron frequency, σ_R is the conductivity of vacuum chamber walls (σ_R =1.1·10^{16} s^{-1} – for stainless steel), and I_0 is the beam current. In the case of zero chromaticity the imaginary part of the tune shift coincides with the instability growth rate. Figure 4 presents the instability growth rates computed with Eq. (6) for the PS-2. The growth rate of the lowest betatron sideband observed at the operating parameters of the FNAL MI is ~0.01 turn^{-1}. As one can see this number is close to the expected growth rates at the PS-2. FNAL uses a digital damper to control the instability. Thus, the usage of similar damper at PS-2 should address the beam stability problem. Note that because of larger ring circumference the instability growth rate at the MI for the Project-X parameters is expected to be ~0.1 turn^{-1} and presents a significant challenge. In both cases the stability at high frequencies should be achieved by using large chromaticity.

Although the use of stainless steel significantly increases the impedance, its value is still at an acceptable level. Thin well-conductive layer (copper or silver) can reduce the impedance at high frequencies but it will not change the impedance significantly at the lowest betatron sideband because its thickness is limited by the field screening discussed in Section 2.

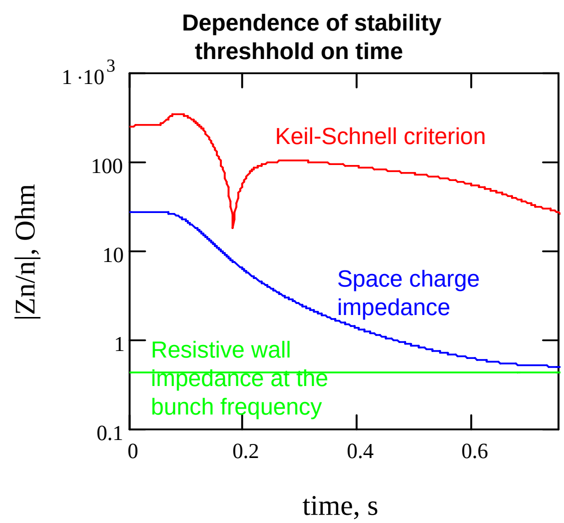

Figure 6. Dependence of the stability criteria on time within accelerator cycle for PS-2 parameters and the stainless steel vacuum chamber.

4. WIDEBAND LONGITUDINAL IMPEDANCE

At low energy and transition crossing, the longitudinal impedance is dominated by the space charge:

$$\frac{Z_n}{n} = i\frac{Z_0}{\beta\gamma^2}\ln\left(\frac{a_y}{1.06\sigma}\right) \quad . \qquad (7)$$

The wall resistivity makes the second largest contribution at small frequencies, f ≤100 MHz,

$$\frac{Z_n}{n} = (1-i)\kappa\frac{Z_0}{4\pi a_y}C\sqrt{\frac{n\omega_0}{4\pi\sigma_R}} \quad . \qquad (8)$$

where κ = 1 and κ = 0.8 for the round and flat vacuum chambers, correspondingly. Figure 5 presents dependence of these impedances on the frequency for the PS-2 parameters and stainless steel vacuum chamber. At high frequencies (f ≥ 100 MHz), similar to the transverse case, the vacuum chamber discontinuities begin dominating the impedance

The wide band longitudinal impedance is sufficiently small and should limit the single bunch longitudinal beam stability as presented in Figure 6.

CONCLUSIONS

There is no doubt that to ensure a reliable operation of the PS-2 with beam current of ~2.5 A one needs to minimize the machine impedances. Nevertheless taking into account that for comparatively short cycle time of ~(1-3) s the eddy currents limit the vacuum chamber conductivity and thickness, and taking into account the mechanical stability of the vacuum chamber, the elliptical stainless steel vacuum chamber still looks as a reasonable choice. Covering it with thin layer of better conducting material (gold, silver or copper) would be helpful but is rather a question of choice than a necessity. To prevent the domination of bending field screening by this layer its thickness should not exceed 30-50 μm. That results in that the full gain in the impedance proportional to $\sqrt{\sigma_1/\sigma_2}$ will only be observed at high enough frequencies, ≥20 MHz. The impedance value at the revolution frequency will be rather set by the limitation on the bending field screening than by conductivity of the material.

To keep the impedance at minimum the standard practice, for reducing discontinuities of the vacuum chamber, needs to be used: good electromagnetic screening of bellows and other discontinuities of the vacuum chamber, careful design of kicker and septum magnets, *etc*.

To guaranty multibunch stability the transverse and longitudinal bunch-by-bunch dampers have to be used.

ACKNOWLEDGEMENTS

The author is grateful to N. Gelfand for careful reading of manuscript and suggestions for its improvements.

REFERENCES

[1] Accelerator Issues of Project X, Fermilab, August 2007; http://projectx.fnal.gov/AACReview/ProjectXAacReport.pdf
[2] A. Burov and V. Lebedev, “Transverse resistive wall impedance for multi-layer round chambers,” EPAC-2002.
[3] A. Burov and V. Lebedev, “Transverse resistive wall impedance for multi-layer flat chambers,” EPAC-2002.
[4] “Run IIA handbook”, FNAL, 2001.